sustainability

MDPI

Article

Analysis of Spatiotemporal Variations in Vegetation Cover and Its Drivers in the Kuye River Basin, Middle Reaches of the Yellow River, China

Jiankang Zhang [1,2,3], Futian Liu [1,2,3], Liangjun Lin [4], Xiaozhong Ding [5], Jiping Wang [6,*], Jing Zhang [1,2,3] and Sheming Chen [1,2,3]

1 Tianjin Center, China Geological Survey, Tianjin 300170, China; jiankangzhang@88.com (J.Z.)
2 North China Center for Geoscience Innovation, China Geological Survey, Tianjin 300170, China
3 Tianjin Key Laboratory of Coast Geological Processes and Environmental Safety, Tianjin 300170, China
4 Center for Hydrogeology and Environmental Geology Survey, China Geological Survey, Tianjin 300309, China
5 Institute of Geology, Chinese Academy of Geological Science, Beijing 100037, China
6 Institute of Ecological Conservation and Restoration, Chinese Academy of Forestry, Beijing 100091, China
* Correspondence: wang_jp@caf.ac.cn

Abstract

Clarifying the dynamic changes in vegetation cover and the driving mechanisms under the combined influence of the natural environment and human activities is a crucial foundation for understanding the evolutionary processes of ecosystems in arid and semi-arid regions and for improving the effectiveness of ecological restoration. Taking the Kuye River Basin, a typical resource exploitation zone in the middle reaches of the Yellow River, as the research area, this study retrieved 30 m resolution annual maximum NDVI datasets from 1986 to 2020 to calculate the Fractional Vegetation Cover (FVC). Utilizing methods such as Theil–Sen slope analysis, Mann–Kendall significance test, Hurst exponent, stability analysis, geographical detector, and sensitivity index, this study systematically revealed the spatiotemporal patterns of vegetation change, future evolution trends, and the response mechanisms of FVC dynamics to multiple factors including climate, topography, and land use. The results indicated that from 1986 to 2020, FVC in the study area exhibited an overall increasing trend (0.0105 a^{-1}), with the average FVC rising from 0.21 to 0.61. Regions with very low and low vegetation coverage continued to decrease, while areas with high and very high vegetation coverage showed significant increases, particularly in the very high vegetation coverage category, which experienced the largest growth (CV = 179.32%). The regions with moderate vegetation coverage demonstrated the highest stability (CV = 48.42%). Analysis of the driving mechanisms revealed that precipitation and land use types were the primary factors influencing changes in FVC, with land use demonstrating a more stable explanatory power (CV = 3.63%). Furthermore, the interaction between these two factors significantly enhanced the explanatory power related to vegetation changes. Sensitivity analysis indicated that the increase in forest and grassland effectively mitigated the negative impact of cropland on moderate to high coverage areas; industrial and mining land had a notable impact on very low coverage areas. It can be inferred that the Grain for Green program and the expansion of industrial and mining lands might generate differentiated impacts across diverse vegetation coverage classes. Future projections indicate that 91.19% of the region exhibits potential for FVC improvement in the future. However, a risk of sustained vegetation degradation exists in densely populated areas and regions with concentrated industrial and mining land. The study demonstrates that under the combined influences of climate change and land use adjustments, optimizing land use structures and coordinating ecological restoration with resource development are critical approaches to

Check for updates

Academic Editor: Anna De Marco

Received: 15 May 2026
Revised: 9 July 2026
Accepted: 13 July 2026
Published: 16 July 2026

Copyright: © 2026 by the authors. Licensee MDPI, Basel, Switzerland. This article is an open access article distributed under the terms and conditions of the Creative Commons Attribution (CC BY) license.

enhancing the stability of ecosystems in arid and semi-arid regions, as well as promoting sustainable regional ecological development.

Keywords: Kuye River Basin; fractional vegetation cover (FVC); spatiotemporal analysis; driving mechanism; geographical detector; land use

1. Introduction

As a crucial component of terrestrial ecosystems, vegetation plays an indispensable role in regulating energy exchange, water circulation, and material cycling [1,2]. It also serves as a critical transitional medium connecting the atmosphere, soil, and water bodies [3]. Fractional Vegetation Cover (FVC) is a core indicator for characterizing surface vegetation status and ecosystem stability, and has been widely applied in research on regional eco-environmental evolution [3,4]. Climate change exerts profound impacts on vegetation growth in arid and semiarid areas, among which precipitation and temperature are the dominant climatic factors controlling the spatiotemporal dynamics of vegetation [5–7]. Future climate shifts are expected to reshape the spatial distribution features of drought-tolerant and drought-avoiding plants [8]. Meanwhile, land use change and human activities, including agricultural expansion and resource exploitation, also impose substantial effects on vegetation variations [9]. Therefore, systematic analysis of FVC change and its underlying driving mechanisms from a multi-factor perspective is essential for clarifying regional ecological evolution processes.

The middle reaches of the Yellow River are influenced by arid climate, complex topography, and long-term human disturbances, resulting in ecologically fragile landscapes, and thus have become a key region for national eco-environmental governance in China [10,11]. As a typical watershed within this region, the Kuye River Basin encompasses diverse landform types, including hilly and gully areas, soft rock (Pisha sandstone) distribution areas, and sandy areas, exhibiting significant spatial heterogeneity in ecological conditions [12,13]. At the same time, this basin is an important energy resource development area in the middle reaches of the Yellow River, where resource exploitation has triggered the continuous expansion of industrial and mining land, profoundly altering regional land use patterns and the ecological environment quality [14]. Since the implementation of a series of ecological restoration projects (represented by the Grain for Green program) in the late 1990s, the overall vegetation condition in the region has been effectively improved [15]. However, under the dual background of ongoing ecological restoration and continuous industrial and mining land expansion, the influences of different land use types on vegetation recovery vary greatly. The mechanisms by which these land use types influence changes in different levels of FVC remain inadequately quantified, presenting a critical scientific bottleneck for a thorough recognition of regional vegetation evolution and the optimization of ecological regulation.

Existing studies have extensively explored the driving mechanisms of vegetation change from perspectives of climate change, human activities, and topographic conditions [16–19], confirming that the dominant influencing factors exhibit significant regional disparities. For example, in the Manas River Basin, the synergistic effect of groundwater and agricultural land is considered the primary driving factor [20]. In the Aksu River Basin, the impact of land use change has surpassed that of climatic factors [21]. In the Chengdu–Chongqing urban agglomeration, vegetation dynamics are collectively governed by climate and human activities [22], and on the Qinghai–Tibet Plateau, temperature, soil type, and elevation have been identified as key factors [23]. These studies indicate that the

driving mechanisms of vegetation change are highly region-dependent. Although relevant research is continuously expanding, limitations remain in terms of temporal scale, spatial resolution, and methodological integration. For instance, long-term series analysis and characterization of staged features are relatively lacking, and systematic research on multi-factor interactions and their spatial response relationships still needs to be strengthened [19]. Moreover, few studies have focused on vegetation dynamics mechanisms under the combined impacts of resource exploitation and ecological restoration. Existing studies have mainly focused on specific areas within the Shen-Dong mining region of the watershed, conducting quantitative analyses of vegetation evolution and driving factors under different disturbance types [24]. In contrast, the Kuye River Basin, located on the southeastern edge of the Mu Us Desert, features complex topography and significant spatial heterogeneity in ecological conditions. As an important coal resource development area, it has long been subjected to the combined effects of intensive mining activities and eco-restoration policies (e.g., the Grain for Green program). At the watershed scale, scholars have not yet formed a comprehensive cognition of the discrepant influences of distinct land use types on different vegetation, as well as their synergistic driving mechanisms in relation to climate, topography, soil, and other factors, particularly in terms of quantitative studies addressing the response features of different levels of FVC. In terms of research methods, existing studies have mostly employed trend analysis, geographic detector, and related statistical methods to analyze vegetation variation and its driving factors [7,9,20,25–27], achieving substantial results across different regions [20,25]. Nevertheless, limitations persist: on the one hand, most studies focused on a single method or a single scale of analysis, with insufficient application of multi-method integration; on the other hand, research on driving factors has largely concentrated on quantifying contributions, while systematic characterization of multi-factor interactions and their spatial response relationships remained relatively limited. Moreover, there is a notable lack of studies addressing the distribution characteristics of vegetation at different stages and their driving mechanisms within the context of long time series analysis.

To address the aforementioned research gaps, this study selected the Kuye River Basin, a typical region featuring concurrent resource exploitation and eco-restoration policies in the middle reaches of the Yellow River, as the study object. This study constructed a long-term dataset of FVC from 1986 to 2020. By integrating multi-source data, including climate, topography, and land use, and utilizing methods such as trend analysis, Hurst exponent, geographic detector, and sensitivity analysis, this research systematically revealed the spatiotemporal patterns of vegetation change, future evolution trends, and their driving mechanisms. The focal points of this study include: (1) the characterization of the long-term spatiotemporal evolution of vegetation coverage and the variation characteristics of different coverage levels; (2) the quantification of the relative explanatory capacities and interaction mechanisms of various factors, both natural and anthropic elements, to vegetation change; and (3) the clarification of the differentiated impacts of ecological restoration projects and changes in industrial and mining land on vegetation dynamics. This research aims to deepen the understanding of vegetation evolution processes and their driving mechanisms in arid and semi-arid regions, providing a scientific basis for land use optimization, ecological restoration, and ecological safety management in resource development areas.

Study Area

The Kuye River is a first-order tributary of the middle reaches of the Yellow River. The basin is geographically situated between 38°23–39°52′ N and 109°28–110°52′ E, covering a total area of approximately 8706 km^2 and spanning Ordos City of the Inner Mongo-

lia Autonomous Region and Yulin City in Shaanxi Province (Figure 1). The basin has a temperate continental climate, with a multi-year average annual precipitation of 386 mm. Precipitation is unevenly distributed throughout the year and exhibits distinct seasonal variation: rainfall is predominantly concentrated in summer, while winter is relatively arid, accompanied by a prominent seasonal temperature difference. As a typical arid and semi-arid watershed, the regional vegetation is mainly composed of dry steppe, deciduous broad-leaved shrubs and psammophytic plant communities. The dominant plant species include *Salix psammophila*, *poplar*, *Stipa bungeana*, *Achnatherum splendens*, *Pinus tabuliformis*, *Caragana korshinskii*, *Hippophae rhamnoides*, *Medicago sativa*, *Psammochloa villosa*, and *Artemisia ordosica*. The Kuye River Basin is a typical ecologically fragile region with intensive resource exploitation activities in the middle Yellow River basin, which plays a vital role in maintaining regional ecological security and soil and water conservation. The study area is located at the transition zone between the southeastern margin of the Mu Us Desert and the Loess Plateau, characterized by complex topography and significant spatial heterogeneity, with elevations ranging from 733 to 1575 m and significant spatial heterogeneity. The central-western part of the basin belongs to the Ordos Plateau, with relatively gentle topographic relief; the eastern part lies at the northern edge of the Loess Plateau, where gullies and ravines are densely distributed and erosion is intense. These distinct geomorphological units collectively create a notable ecological environment gradient across the basin. The basin is characterized by a widespread distribution of industrial and mining land, and long-term resource exploitation has substantially altered regional land use patterns, which have had a lasting impact on the evolution of the regional ecological environment. Since the late 1990s, the national government of China have rolled out a series of large-scale eco-rehabilitation initiatives one after another, including the Three-North Shelter Forest Program and the Grain for Green program. Consequently, regional vegetation coverage has steadily increased, with average vegetation cover surpassing 60% in recent years. At present, grassland accounts for 60% of the study area, cultivated land makes up 17%, industrial and mining land occupies 6%, and all other land use types account for relatively small proportions. The long-term spatial and temporal overlap of resource exploitation and ecological restoration has made the Kuye River Basin a typical representative area for investigating the combined impacts of natural and human disturbances on vegetation variations and their response mechanisms.

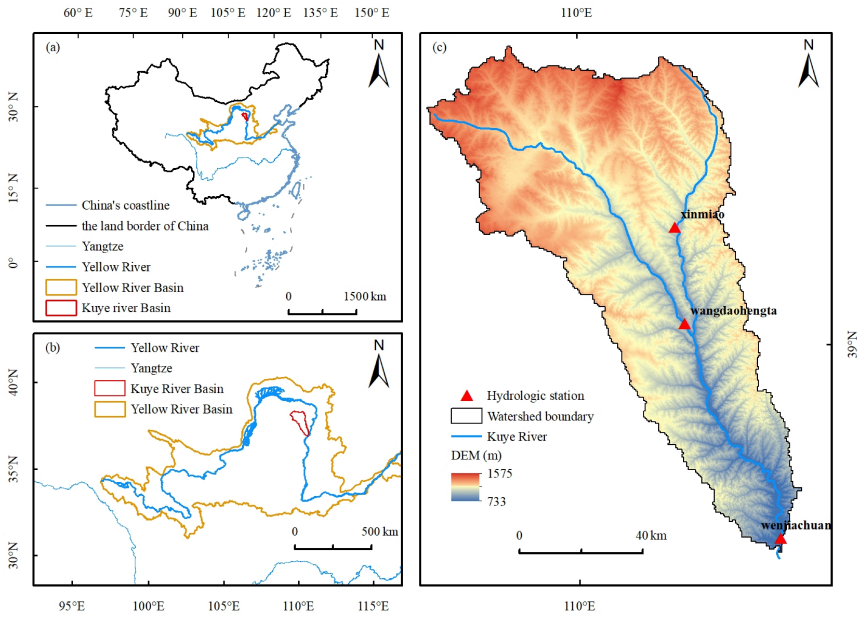


Figure 1. Location of the study area: (**a**) China; (**b**) Yellow River Basin; (**c**) Kuye River Basin.

2. Data and Methods

2.1. Data Sources and Processing

The data used in this study include fractional vegetation cover, meteorological data, digital elevation model (DEM), land use, and soil type. Vegetation data was sourced from the Resource and Environmental Science Data Center (https://www.resdc.cn/). The data was derived from the Google Earth Engine (GEE) remote sensing platform, utilizing remote sensing imagery from the Landsat 5 and 8 satellites to calculate annual maximum NDVI datasets from 1986. All data processing and preprocessing procedures were completed by the data provider. For the whole computation procedure, NDVI values were generated from every Landsat 5 and 8 image covering each year, and the maximum annual NDVI corresponding to each raster pixel was extracted from the entire year's data, resulting in the generation of annual maximum NDVI datasets. For the NDVI calculation from Landsat 5, bands 4 and 3 were utilized, while for Landsat 8, bands 5 and 4 were applied. Fractional vegetation cover (FVC) was retrieved using the pixel dichotomy model based on the annual maximum normalized difference vegetation index (NDVI). Meteorological data, including annual precipitation and annual mean temperature, were obtained from the National Tibetan Plateau Science Data Center (http://data.tpdc.ac.cn/). These data were derived from monthly precipitation and temperature data by accumulation or averaging, spanning 1986–2020 at a spatial resolution of 1000 m. DEM data were sourced from the ASTER GDEM dataset provided by the geospatial data cloud platform (https://www.gscloud.cn/), with a spatial resolution of 30 m. Land use data were provided by the Institute of Geographic Sciences and Natural Resources Research, Chinese Academy of Sciences, for the years 1980, 1990, 2000, 2010, and 2020, at a spatial resolution of 30 m. Soil data were obtained from the National Soil Science Data Center at a spatial resolution of 90 m (https://soil.geodata.cn/ztsj.html, accessed on 12 August 2025). Additionally, population density data, used to assist in analyzing human activity impacts, were sourced from the National Earth System Science Data Center for the years 2000, 2010, and 2020, with a spatial resolution of 100 m (https://www.geodata.cn/main/, accessed on 12 August 2025). To ensure consistency among multi-source data, all datasets were uniformly resampled to a 30 m spatial resolution and underwent coordinate system unification and spatial registration. Data processing and analysis were primarily performed using ArcGIS 10.8, ENVI 5.2, Python 3.11 and Origin 2024.

2.2. Methods

2.2.1. Fractional Vegetation Cover

Fractional vegetation cover (FVC) is a commonly used indicator for characterizing surface vegetation conditions. To obtain the FVC dataset in this study, this study applied the pixel dichotomy model [28]:

$$\mathrm{FVC} = \frac{NDVI - NDVI_{soil}}{NDVI_{max} - NDVI_{soil}} \quad (1)$$

where $NDVI_{soil}$ and $NDVI_{max}$ represent the NDVI values of pure bare soil pixels and pure vegetation pixels, respectively. Referring to existing studies, utilizing the 5% and 95% of the cumulative distribution of NDVI as thresholds for bare soil and pure vegetation pixels, respectively, effectively mitigates the interference caused by image noise and outliers [29,30]. Based on the FVC values, vegetation coverage was classified into five levels: very low (<0.1), low (0.1–0.3), medium (0.3–0.5), high (0.5–0.7), and very high (>0.7).

2.2.2. Theil–Sen Slope and Mann–Kendall Significance Tests

This research adopted the Theil–Sen slope estimator to quantify long-term FVC changes in the Kuye River Basin from 1986 to 2020, while the Mann–Kendall significance test was introduced to judge whether these temporal trends reach statistically remarkable levels. The combined application of these two statistical testing methods effectively mitigates the interference caused by NDVI outliers [31]. The Theil–Sen slope test computes slope coefficients for every two paired records in the time sequence, and takes the median of all slopes as a representative trend for the overall temporal change, with the computational equation shown below:

$$Slope = Median\left(\frac{FVC_{\mathrm{j}} - FVC_i}{j - i}\right), \forall \mathrm{j} > i \tag{2}$$

This median slope acts as the core representative metric of all pairwise slope results. Positive median values correspond to ascending vegetation restoration tendencies, whereas negative values imply descending vegetation degradation trends. Here, FVC_i and FVC_j denote the FVC values in year i and year j within the time series, and the Median operator extracts the middle value among all pairwise slope outputs.

To further analyze the temporal variation trend of FVC, the Mann–Kendall significance test was applied in this work to verify the statistical reliability of time-series trends. The relevant calculation formula is as follows [32]:

$$Z = \begin{cases} \frac{S-1}{\sqrt{\frac{n(n-1)(2n+5)}{18}}}, S > 0 \\ 0, S = 0 \\ \frac{S+1}{\sqrt{\frac{n(n-1)(2n+5)}{18}}}, S < 0 \end{cases} \tag{3}$$

$$S = \sum_{\mathrm{i}=1}^{\mathrm{n}-1} \sum_{\mathrm{j}=\mathrm{i}+1}^{\mathrm{n}} sign(FVC_{\mathrm{j}} - FVC_i) \tag{4}$$

$$sign(FVC_{\mathrm{j}} - FVC_i) = \begin{cases} 1, FVC_{\mathrm{j}} - FVC_i > 0 \\ 0, FVC_{\mathrm{j}} - FVC_i = 0 \\ -1, FVC_{\mathrm{j}} - FVC_i < 0 \end{cases} \tag{5}$$

In the above formulas, n denotes the total number of time-series samples; *sign* refers to the sign function in mathematics. FVC_i and FVC_{j} separately represent FVC raster data collected at two distinct time points for trend detection. In this study, trend results are identified as statistically significant at $\alpha = 0.05$ ($|Z| > 1.96$) and extremely significant at $\alpha = 0.01$ ($|Z| > 2.58$).

In addition, the FVC trend slopes derived from Theil–Sen estimation and Z statistics from Mann–Kendall testing were combined to quantitatively characterize the statistical reliability of FVC temporal shifts over the Kuye River Basin (1986–2020). All FVC dynamic patterns were further divided into six classification levels [33]: extremely significant increasing, significant increasing, slight increasing, slight decreasing, significant decreasing, and extremely significant decreasing.

2.2.3. Hurst Exponent

The Hurst exponent was adopted to forecast the prospective changing trajectories of fractional vegetation cover (FVC) across the Kuye River Basin. First proposed by British hydrologist Hurst in 1965, the Hurst exponent has been extensively applied within geographical research to quantify the self-similar characteristics and long-range correlation embedded in time-series raster datasets [34,35]. Rooted in the rescaled range (R/S) ana-

lytical framework, this indicator quantifies the temporal evolutionary signatures of FVC time series. When 0 < H < 0.5, the time sequence displays anti-persistent characteristics, signifying that the forthcoming vegetation tendency will reverse its historical trajectory. In contrast, 0.5 < H < 1 denotes persistent behavior, meaning the future vegetation dynamic will follow the previous changing pattern. Moreover, the persistence strength intensifies as H approaches 1 [36]. The computational formulas for the Hurst exponent are displayed below:

$$\frac{R_\tau}{S_\tau} = c\tau^H \tag{6}$$

$$R_\tau = \max_{1\le t\le\tau} X(t,\tau) - \min_{1\le t\le\tau} X(t,\tau) \tag{7}$$

$$S_\tau = \sqrt{\frac{1}{\tau}\sum_{t=1}^{\tau}\left(FVC_t - \overline{FVC_\tau}\right)^2} \tag{8}$$

$$X_{(t,\tau)} = \sum_{j=1}^{t}\left(FVC_t - \overline{FVC_\tau}\right)\ (1 \le \mathrm{t} \le \tau) \tag{9}$$

$$\overline{FVC_\tau} = \frac{1}{\tau}\sum_{t=1}^{\tau} FVC_t\ (\tau = 1,\ 2,\ 3, \ldots,\ \mathrm{n}) \tag{10}$$

In these equations, H stands for the Hurst exponent, R_τ represents the rescaled range, and S_τ refers to the standard deviation. $X_{(t,\tau)}$ denotes the cumulative deviation sequence, FVC_t corresponds to the FVC value in the t-th year, and $\overline{FVC_\tau}$ indicates the average FVC value over the entire time series. To further dissect the prospective variation trends of FVC over the Kuye River Basin, this study integrated the interannual FVC trend slopes and Hurst exponent values to carry out comprehensive joint analysis [37]. The classification criteria for combined trend-persistence types are summarized in Table 1, which facilitates the generation of spatial maps revealing the coupled patterns of FVC evolutionary trends and their persistence features.

Table 1. Classification of FVC future trends.

S_{FVC}	H	FVC Future Trend
>0	>0.5	Sustained increasing
>0	<0.5	Decreasing from increasing
<0	>0.5	Sustained decreasing
<0	<0.5	Increasing from decreasing

2.2.4. Stability Analysis

Defined as the quotient between standard deviation and data mean, the variation coefficient is widely applied to describe the stability and oscillating traits of time-series data [38]. This study utilized the Coefficient of Variation (CV) to characterize the temporal stability of FVC sequences in this research [20]. The corresponding computational equation is shown below:

$$CV = \frac{\sigma}{\mu} \times 100\% \tag{11}$$

In this formula, σ denotes standard deviation, which quantifies data dispersion; μ is the mean value that reflects data central tendency. Higher CV indicates significant fluctuations in the FVC fluctuations. Conversely, a lower CV suggests smoother fluctuations in the FVC data, indicating more stable vegetation growth conditions.

2.2.5. Geographical Detector

The geographical detector is a statistical approach for detecting spatial stratified heterogeneity and revealing its underlying driving forces. The core theory lies in evaluating the spatial matching degree between independent and dependent variables based on

spatial heterogeneity. This model has been extensively adopted to reveal the driving mechanisms behind various geographical variables [7,9] and encompasses four modules: factor, ecological, interaction, and risk detection. In this study, the factor and interaction detection modules were selected to explore the driving factors affecting FVC variations across the Kuye River Basin. Previous research on the driving mechanisms of vegetation cover change has utilized correlation analysis or scenario simulation evaluation methods; however, these approaches may be less efficient when dealing with multiple influencing factors. The geographic detector effectively overcomes this issue, and for its underlying principles [39].

Factor detection requires first detecting the spatial stratified heterogeneity of the dependent variable Y, followed by quantifying the explanatory power of each independent factor X for Y, which is represented by the q value. The formula is expressed as

$$q = 1 - \frac{\sum_{h=1}^{L} N_h \sigma_h^2}{N_{\sigma^2}} = 1 - \frac{S_{SW}}{S_{ST}} \quad (12)$$

where h stands for the stratification of the Y and X variables; N_h and N separately represent the sample quantity within the h layer and the whole research area; σ_h^2 and σ^2 refer to the variance of Y values in layer h and the overall regional variance; and SSW and SST correspond to the sum of variances inside each stratification layer and the total regional variance, respectively. The q statistic quantifies how much variance of Y can be explained by X, ranging from 0 to 1. Larger q values signify a stronger explanatory capacity of X over the dependent variable Y.

The interaction detection module is adopted to quantify how multiple driving factors (Xs) jointly affect FVC variations in the study area. Taking X_1 and X_2 as examples, it evaluates whether the explanatory power for Y increases, decreases, or remains mutually independent when X_1 and X_2 act jointly. The computational procedures are listed below. First, the individual explanatory coefficients q(X_1) and q(X_2) are calculated, followed by solving the interaction statistic q($X_1 \cap X_2$). By contrasting the three values q(X_1), q(X_2) and q($X_1 \cap X_2$), the interaction results can be classified into several categories (Table 2).

Table 2. Types of the interaction results.

Interaction Criteria	Interaction Types
$q(X_1 \cap X_2) < min(q(X_1), q(X_2))$	Nonlinear-weakening
$min(q(X1), q(X2)) < q(X1 \cap X2) < max(q(X1), q(X2))$	Univariate-weakening
$q(X1 \cap X2) > max(q(X1), q(X2))$	Bivariate-enhancement
$q(X1 \cap X2) = q(X1) + q(X2)$	Independent
$q(X1 \cap X2) > q(X1) + q(X2)$	Nonlinear-enhancement

Combined with the field characteristics of the research watershed, eight explanatory indicators were screened in this paper to distinguish the core drivers controlling the spatial differentiation of FVC, including land use type, annual average temperature, annual precipitation, soil type, altitude, aspect, slope and population density. The land-use data were classified into seven distinct types: cropland, forestland, grassland, water bodies, residential areas, industrial and mining land, and unused land. Soil types were classified into nine categories: aeolian sandy soil, loessal soil, dark loessial soil, chestnut soil, calcareous regosol, fluvo-aquic soil, meadow soil, bog soil and saline–alkali soil. Utilizing the natural breakpoint method, average temperature, average rainfall, and elevation were classified into six classes, while population density was categorized into ten classes. For slope aspect, the classifications included flat land, north, northeast, east, southeast, south, southwest, west, northwest, and north, totaling 10 classes. Slope gradients were classified

into six types: 0–5°, 5–10°, 10–15°, 15–20°, 20–25°, and >25°. Elevation was grouped into six intervals: <1000 m, 1000–1100 m, 1100–1200 m, 1200–1300 m, 1300–1400 m, and >1400 m. A regular 1 km × 1 km fishnet grid was first generated in ArcGIS. The raster values of FVC and all drivers were then extracted to the grid nodes of the fishnet for subsequent Geographical detector analysis.

2.2.6. Sensitivity Index of FVC to Land Use Change

To quantify how strongly FVC responds to different land-use types, the elasticity coefficient model originating from economic theories [40] was adopted for sensitivity calculation [40].

$$CS = \left| \frac{(FVC_j - FVC_i)/FVC_i}{(X_j - X_i)/X_i} \right| \quad (13)$$

where CS is the sensitivity index, FVC_i and FVC_j separately represent the FVC area proportion in the initial year and the subsequent year, respectively, and X_i and X_j correspond to the area proportions of land use type in the initial year and the subsequent year, respectively. This analysis quantifies the degree of response of vegetation cover to each land use type, which helps thoroughly reveal how susceptible vegetation cover is to external land surface disturbances.

3. Results

3.1. Spatiotemporal Variation in the FVC

3.1.1. Analysis of Spatiotemporal Variation in the FVC

From 1986 to 2020, the fractional vegetation cover (FVC) in the Kuye River Basin generally exhibited a continuous increasing trend. The annual mean FVC fluctuated between 0.21 and 0.61, with a multi-year average of 0.37, showing a significantly increasing trend overall and a linear growth rate of 0.0105 a^{-1} (Figure 2). Spatially, FVC in different years consistently showed a pattern of increasing from northwest to southeast (Figure 3). Areas with high and very high coverage were mainly concentrated in the southeastern part of the basin, with scattered distribution in localized areas of the northwestern part. Areas with low and medium coverage were primarily distributed in the north-central part of the basin and in some regions with relatively intensive human activities.

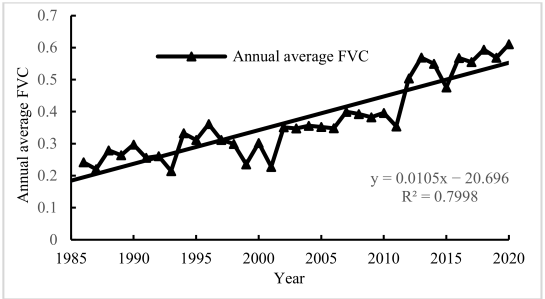


Figure 2. Temporal changes in FVC.

In terms of changes in areal composition (Figure 4), low coverage dominated the basin during 1986–2000, accounting for 74.91%, 58.34%, and 54.93%, respectively. The proportion of medium coverage increased from 18.74% to 37.51%. In 2010, medium coverage accounted for the highest proportion (55.81%) and became the dominant type. By 2020, the proportions of high and very high coverage reached 46.74% and 30.64%, respectively, together exceeding 77%, while the areas of low and very low coverage fell to less than 5%. Stability analysis (Table 3) showed that the areas of all FVC classes exhibited strong

fluctuations (48.42–179.32%), among which the very high coverage area had the largest coefficient of variation (179.32%), while medium coverage was the most stable (48.42%).

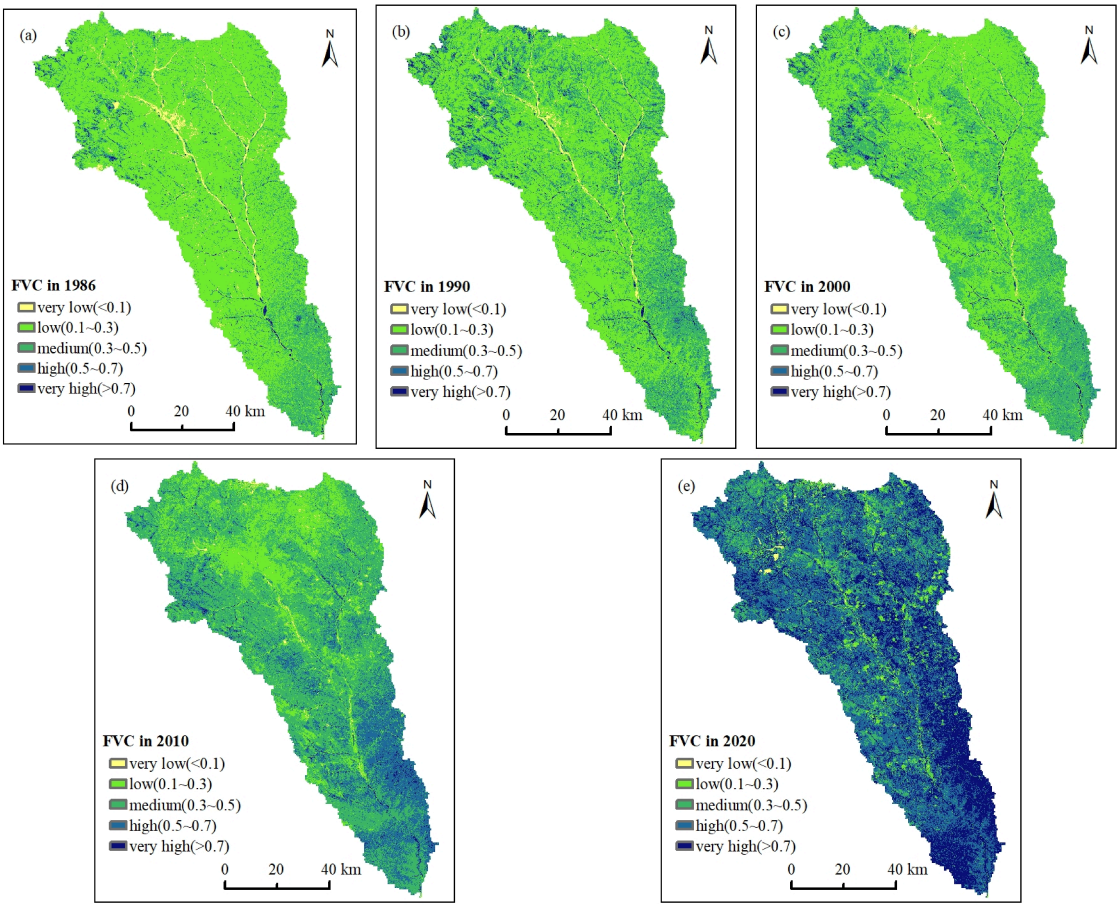


Figure 3. Spatial distribution of FVC in (**a**) 1986; (**b**) 1990; (**c**) 2000; (**d**) 2010; (**e**) 2020.

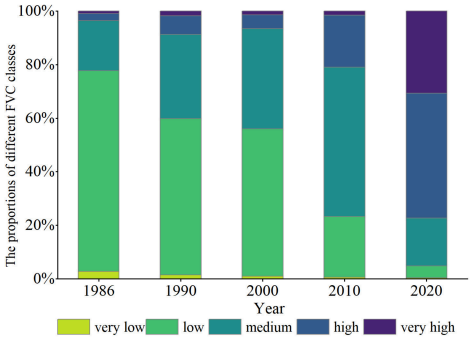


Figure 4. The proportions of different FVC classes.

Table 3. Coefficient of variation in area for different FVC classes (1986–2020).

FVC	Very Low (0–0.1)	Low (0.1–0.3)	Medium (0.3–0.5)	High (0.5–0.7)	Very High (0.7–1)
CV	77.98%	66.57%	48.42%	113.11%	179.32%

The FVC trends, together with their statistical significance across the Kuye River Ba-sin from 1986 to 2020, are shown in Figure 5 and Table 4. As illustrated in Figure 5a,b, the interannual variation slope of FVC within the watershed fluctuated between −0.0266 and 0.0386 a^{-1}. Zones with significant and extremely significant increasing trends accounted for

2.86% and 89.20% of the study area. In contrast, land marked by significant and extremely significant decreasing trends only occupied 0.36% and 0.52% of the study area. Overall, the spatial extent of regions undergoing vegetation recovery far exceeded that of areas suffering vegetation degradation.

Table 4. Classification of FVC changing trends in the Kuye River Basin from 1986 to 2020.

FVC Changing Trends	Proportion	Area (km^2)
extremely significant decreasing	0.52%	44.56
significant decreasing	0.36%	31.05
slight decreasing	2.14%	184.91
extremely significant increasing	89.20%	7704.61
significant increasing	2.86%	246.79
slight increasing	4.93%	425.53

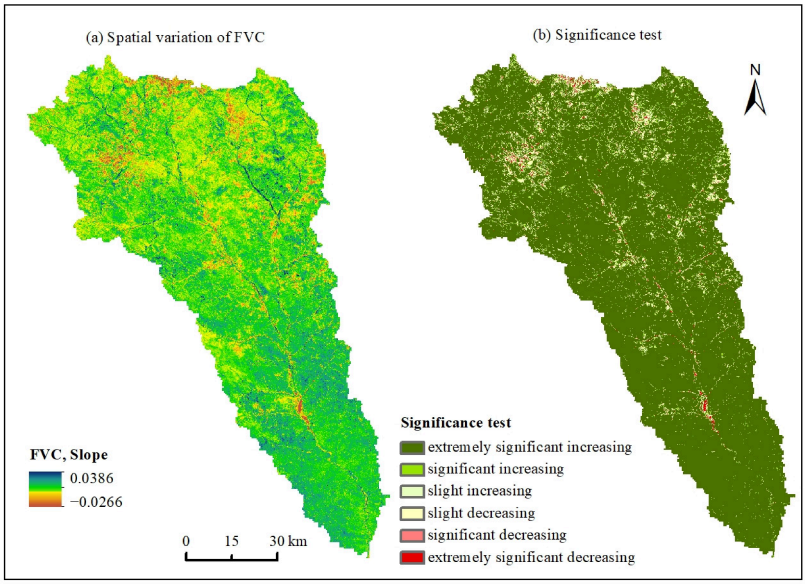


Figure 5. FVC change trend and significance test in the Kuye River Basin between 1986 and 2020: (**a**) spatial variation in FVC, (**b**) significance test.

The trend analysis results (Figure 5 and Table 4) indicated that from 1986 to 2020, approximately 96.98% of the basin area experienced a growth trend in FVC, among which extremely significant increasing areas accounted for 89.20%. Conversely, areas with decreasing trends in FVC covered 260.52 km^2, representing 3.02%. These decreasing trends were predominantly observed in densely populated areas in the northern basin, including Ejin Horo Banner, Dongsheng District and Jungar Banner, as well as in industrial and mining land areas upstream of Shenmu City. The significance test results indicated a significantly increasing trend in FVC within the study area.

3.1.2. Future Projections of FVC

To comprehensively understand the future trends of FVC in the Kuye River Basin, a coupling analysis of the temporal raster trends of FVC and the Hurst exponent was conducted. This analysis produced spatial distributions that combine the future trends and persistence characteristics of FVC.

It can be observed from Figure 6 that the future trends of FVC in the Kuye River Basin are predominantly characterized by sustained increasing. However, increasing and decreasing trends are interwoven, displaying notable spatial heterogeneity. Densely populated areas in the northern basin, including Ejin Horo Banner, Dongsheng District

and Jungar Banner, as well as industrial and mining land zones upstream of Shenmu City, remain at risk of sustained decreasing. Across the entire basin, various trends are interspersed, but increasing trends remain dominant. According to Table 5, the proportion of areas transitioning from increasing to decreasing is 5.97%, while areas transitioning from decreasing to increasing account for 0.18%. Areas with sustained decreasing account for 2.83%, and areas with sustained increasing make up 91.01%.

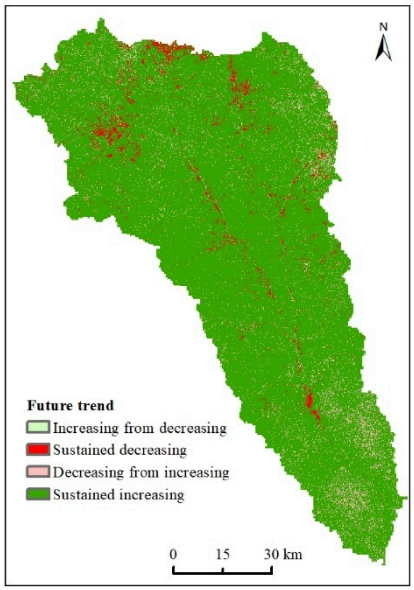


Figure 6. Spatial distribution of future predictions of FVC on the Kuye River Basin.

Table 5. Statistical results of FVC trends on the Kuye River Basin.

FVC Future Trend	Proportion	Area (km^2)
Increasing from decreasing	0.18%	15.54
Sustained decreasing	2.83%	244.55
Decreasing from increasing	5.97%	515.61
Sustained increasing	91.01%	7860.51

3.2. Geographical Detection of Factors Influencing the FVC

3.2.1. Factor Detection

This study adopted factor detection to quantify the explanatory capacity of each selected factor for FVC spatial patterns in 1986, 1990, 2000, 2010 and 2020. The results can be found in Figure 7. In the study area, land use type and precipitation exhibited higher explanatory power for the spatial distribution of FVC when compared to other factors. The maximum explanatory power of precipitation for FVC reached 0.26, while the explanatory power of land use for FVC remained approximately 0.11 across all periods. The multi-year average results (Figure 7f) revealed the ranking of explanatory strength of the selected elements on the FVC as listed below: annual precipitation > land use types > annual mean temperature > soil type > altitude > slope > population density > aspect. The explanatory powers of precipitation (q = 0.115) and land use types (q = 0.1097) for the spatial distribution of FVC were relatively high, suggesting their superior influence on FVC within the study area. By contrast, slope, aspect and population density exhibited relatively weak explanatory power, indicating their lower influences on regional FVC. The *p*-value reflects the statistical significance of each driving factor. When the *p*-value falls below 0.05, the factor shows statistically significant difference; values smaller than 0.01 correspond to extremely significant differences. Nearly all impact factors yielded a *p*-value equal to 0,

which pointed to extremely significant difference from FVC, while the slope aspect factor had a *p*-value exceeding 0.05 in 1986, indicating an insignificant influence on FVC.

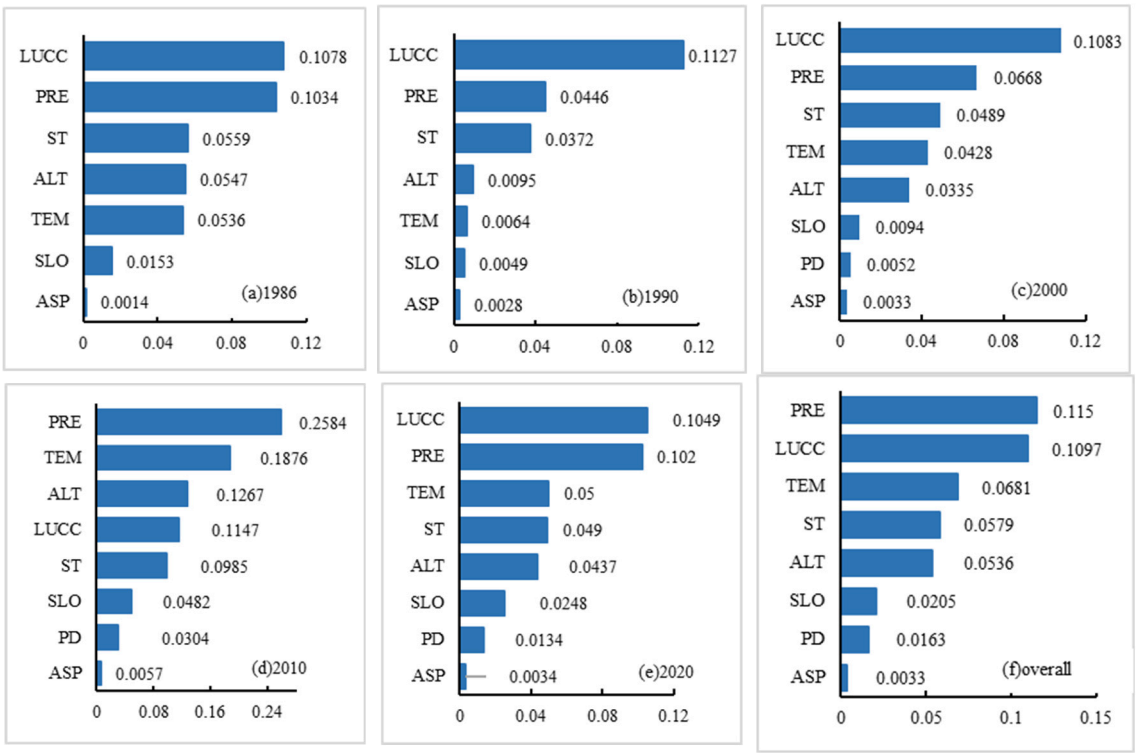


Figure 7. Distribution of q-values of influencing factors for FVC change across the years.

The analysis of the coefficient of variation in q-values (Table 6) showed that the stability of different factors varied significantly. Among them, land use type exhibited the smallest variation (CV = 3.63%), indicating relatively high stability, while precipitation showed larger variation (CV = 72.94%), indicating relatively low stability.

Table 6. Coefficient of variation in q-values for influencing factors.

Influencing Factor	Annual Mean Temperature	Slope	Elevation	Population Density	Annual Precipitation	Aspect	Soil Type	Land Use Type
CV	101.95%	83.77%	82.32%	78.91%	72.94%	47.15%	40.85%	3.63%

3.2.2. Interaction Detection

As illustrated in Figure 8, this study quantified interactive relationships among FVC impact factors in 1986, 1990, 2000, 2010, and 2020. Every combination of explanatory variables generated enhanced explanatory capacity. The proportion of non-linear enhancement interaction results reached a maximum of 95.24%, indicating that the variation in FVC values mostly arises as a consequence of interactive coupling effects from multiple factors. In each of the years analyzed, the combination ranking first in the intensity of interactive effects was consistently land use type∩annual precipitation, with the maximum value of q = 0.3296. The results of these interaction detections further confirmed that land use type and annual precipitation had the strongest explanatory power for the spatial distribution of FVC in the Kuye River basin. In conclusion, the two-factor interactions were not simple superposition effects; instead, they manifested as bivariate nonlinear enhancement relationships.

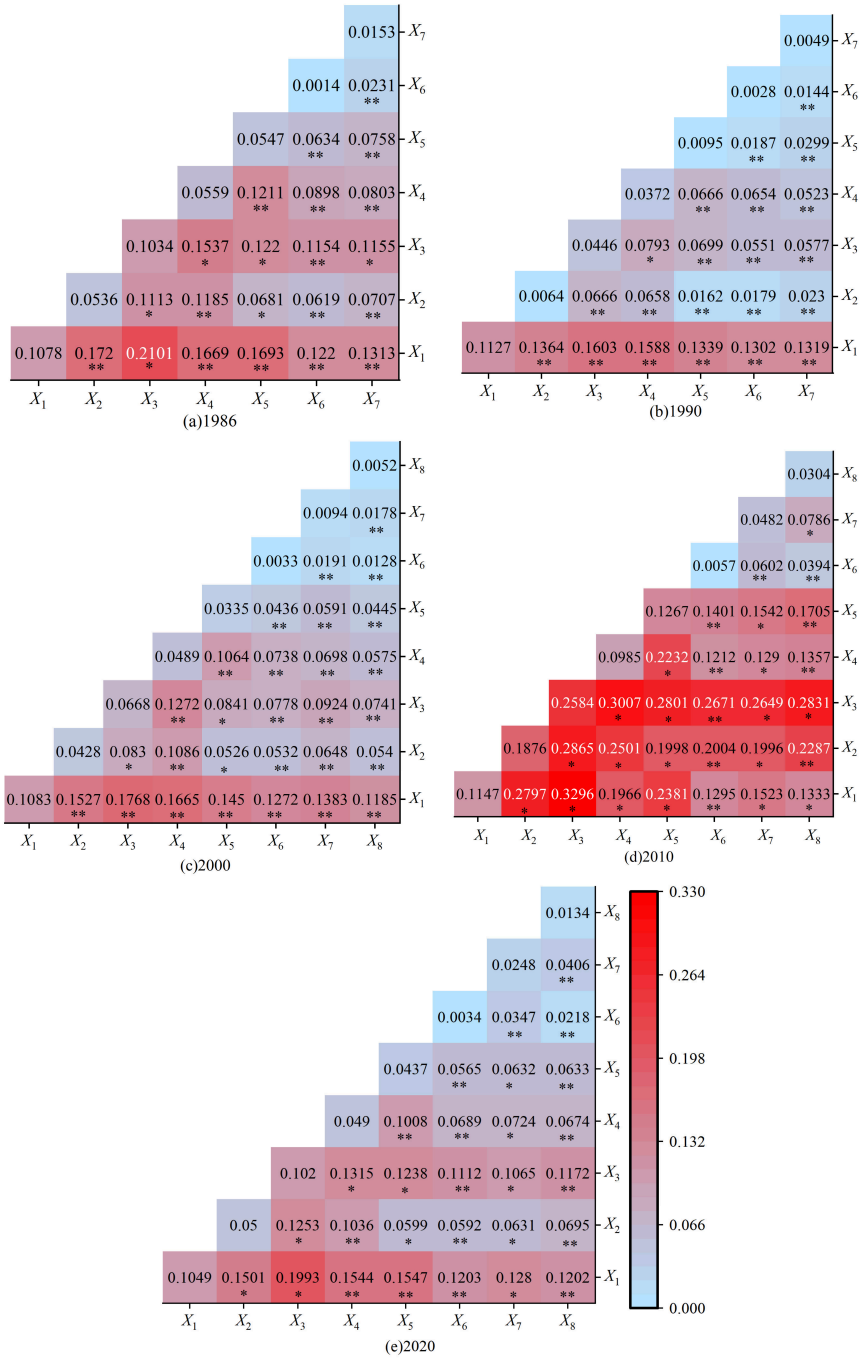


Figure 8. Interaction detection among factors influencing FVC change (*: two-factor enhancement; **: nonlinear enhancement). X_1: Land use type; X_2: Annual mean temperature; X_3: Annual precipitation; X_4: Soil type; X_5: Altitude X_6: Aspect; X_7: Slope; X_8: Population density.

3.3. Sensitivity Response Characteristics of Fractional Vegetation Cover to Different Land Use Types in the Kuye River Basin

To quantify the response characteristics of fractional vegetation cover (FVC) to major land use types over different time periods, this study employed the elasticity coefficient method to analyze the sensitivity of cropland, forestland, grassland, and industrial and mining land to different FVC classes from 1986 to 2020 (Figure 9). The results show that industrial and mining land exhibited the highest sensitivity to very low coverage areas (0–0.1), and reached a peak of 16.84 after 2010. Medium coverage areas (0.3–0.5) were mainly influenced by cropland, with the highest sensitivity index of 10.53 during 2000–2010. High coverage areas (0.5–0.7) were increasingly affected by cropland and forestland, with

sensitivity indices reaching 5.05 and 3.75, respectively, in 2020. Grassland had a notable impact on low coverage areas (0.1–0.3), with a sensitivity index of 3.37 during 1990–2000. In very high coverage areas (0.7–1), forestland exerted the most pronounced influence, with relatively high sensitivity indices during both 1990–2000 and 2010–2020. Overall, different land use types exhibited distinct sensitivities to FVC, with dynamic changes across stages: industrial and mining land mainly affected very low coverage areas, grassland influenced low coverage areas, cropland influenced medium coverage areas and forestland affected high and very high coverage areas. These results revealed the spatiotemporal response characteristics of land use types to vegetation cover.

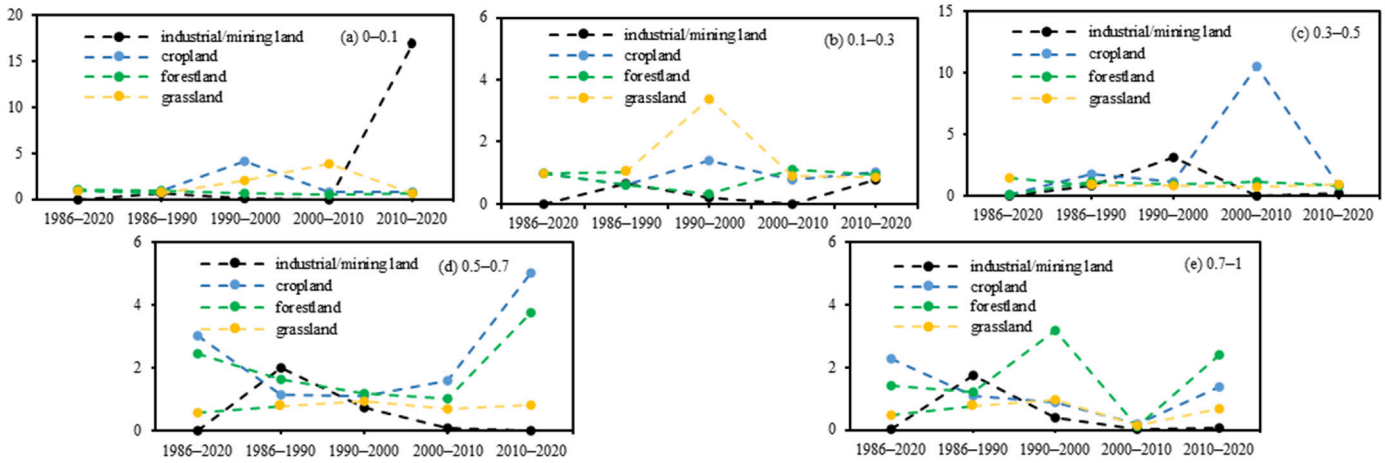


Figure 9. Changes in vegetation cover on cropland, forestland, grassland, and industrial/mining land.

4. Discussion

4.1. Spatiotemporal Variation in Vegetation Cover

Previous studies have shown that the multi-year mean NDVI in the Kuye River Basin has exhibited a fluctuating upward trend since 2000, with a spatial pattern increasing from north to south [12]. This study further reveals the characteristics of FVC change in the study area from 1986 to 2020. Overall, the annual average FVC increased at a rate of 0.0105 a^{-1}, peaking in 2020, with 96.98% of the area showing an increasing trend. Different coverage classes exhibited clear regularities: very low and low vegetation coverage continued to decrease, while high and very high coverage increased significantly, with very high coverage showing the largest increase (CV = 179.32%). Medium coverage was the most stable (CV = 48.42%). Spatially, regions with high and extremely high FVC were predominantly concentrated in the southeastern part and some areas of the northwestern part (Ejin Horo Banner, Kangbashi District); very low coverage was distributed in densely populated areas and along river courses. The coexistence of very low and very high coverage in Ejin Horo Banner may be related to industrialization and urbanization processes [41–43]. Overall, the ecological environment of the basin improved significantly from 1986 to 2020, which aligns with research outcomes on the Yellow River Basin [11,15,19], the Yanhe River [10], the Jinghe River [44], and Shaanxi Province [25].

In addition, the Hurst exponent analysis, reliant on spatial autocorrelation of long-term raster datasets, suggested that 91.19% of the region exhibits potential for FVC improvement in the future. However, there remains a risk of sustained vegetation degradation in densely populated areas and regions with concentrated industrial and mining land. This result indicates that ecological governance in the Kuye River Basin requires balancing economic development and ecological resilience, and it is essential to emphasize the long-term relationship between resource exploitation and vegetation coverage. Notably, Hurst exponent calculation merely utilizes temporal FVC records and does not take full account of other

impact variables such as temperature, precipitation and human activities [45]. Vegetation changes are highly sensitive and dependent on multiple natural and anthropogenic factors [46], which implies certain limitations in the trend analysis methods mentioned above. Accordingly, it is necessary to incorporate multiple drivers in the future to improve the accuracy of predictions of regional vegetation restoration.

4.2. Driving Factors of Spatiotemporal Variation in Vegetation Cover

Geographic detector analysis showed that vegetation change in the Kuye River Basin was driven by both natural and anthropogenic factors, with precipitation and land use type being the primary factors. The multi-year mean q-value of annual precipitation (0.115) was slightly higher than that of land use type (0.1097), but precipitation exhibited large fluctuations (CV = 72.94%), whereas land use type was more stable (CV = 3.63%), indicating that meteorological factors cause short-term fluctuations in FVC, while land use exerted a robust role over the long term. Temperature, topography, and population density also imposed certain effects on FVC: temperature facilitated vegetation growth; elevation and slope influenced vegetation distribution by modulating temperature, precipitation, and soil conditions [18,47,48]. Although population density presented a relatively weak overall influence on FVC, its driving capacity displayed an increasing trend since 2000, reflecting increased pressure on local vegetation due to urbanization [49–51]. These findings were consistent with studies on the Loess Plateau, Yanhe River Basin, and Jinghe River Basin [10,44,52,53], but contrasted with the groundwater–agriculture synergy in the Manas River Basin [20] and the dominance of land use in the Aksu River Basin [21], indicating that the intensity of resource exploitation and the context of ecological engineering jointly regulated vegetation response mechanisms.

Interaction analysis showed that all factor pairs exhibited two-factor enhancement, and most presented nonlinear enhancement. Among all factor combinations, the joint effect of land use types and annual precipitation delivered the most powerful interpretation for regional FVC spatial patterns across the study basin, indicating that anthropogenic activities can amplify the impact of meteorological factors on vegetation [26,54,55]. Therefore, FVC change was the result of multi-factor interactions in which land use type provided stable driving, precipitation dominated short-term fluctuations, and the interaction between meteorological and anthropogenic factors enhanced vegetation restoration effects. These analytical findings provide a theoretical basis for subsequent analysis of the sensitivity of different land use types to various FVC classes.

This study confirmed that land use was the dominant anthropogenic factor affecting vegetation cover change, which was consistent with previous findings [12]. However, previous studies did not clarify how different land use types alter vegetation cover. Sensitivity analysis revealed that different land use types exhibited hierarchical differences in their response to FVC change: grassland was sensitive to low-coverage areas, cropland to medium-coverage areas, forestland to high and very high coverage areas, and industrial and mining land to very low coverage areas, with the impact reaching its peak during 2010–2020. This conclusion was closely aligned with the execution scheme of the Grain for Green program carried out in the study area. The increase in forest and grassland effectively reduced the negative impact of cropland on medium-to-high coverage areas, strengthened the positive effects of forestland and grassland on vegetation restoration, and greatly improved the local eco-environment of the study area. Industrial and mining land had a significant impact on very low coverage areas (0–0.1), with the sensitivity index for very low coverage areas reaching 16.84 during 2010–2020, indicating increased sensitivity of very low coverage areas to industrial and mining land, while high coverage areas showed enhanced resilience to mining development. These results suggest that a comprehensive

land-ecological management strategy should be implemented in and around mining areas, balancing economic development and ecological resilience, with attention to the sustained relationships linking industrial/mining land to vegetation cover.

Overall, vegetation change in the Kuye River Basin could be attributed to coupling among climatic factors (precipitation, temperature), topographic conditions (altitude, slope), land use types, and human engineering. Precipitation and land use constituted the primary driving factors underlying the spatial heterogeneity of vegetation, with their interaction enhancing the driving effect. The Grain for Green program and mining area management might stand out as core factors facilitating vegetation recovery in recent periods. This mechanistic analysis not only enriched insights into vegetation change patterns in arid and semi-arid regions but also delivered theoretical and scientific references for eco-reconstruction and resource management in the Yellow River Basin.

4.3. Innovation and Shortcomings

Existing research has investigated the spatiotemporal variations in vegetation coverage and their driving forces within the Kuye River Basin [12], However, those studies only quantified the single-factor driving effects of climate or human activities. The existing literature has largely adopted correlational and regression statistical techniques. These tools perform well in depicting links between continuous variables and calculating spatial heterogeneity at small regional scales. Instead of adopting conventional statistical approaches, this study applied a novel spatial statistical method, namely the geographical detector model, to quantify how FVC interacts with its driving factors within the Kuye River Basin, and found that it exhibited an interactive enhancement effect. This study found that land use type has a more stable explanatory power for FVC change over the long term, and revealed the differentiated roles of different land use types (cropland, forestland, grassland, industrial/mining land) across different vegetation coverage classes. By calculating the sensitivity of different FVC classes to various land use types, an elastic relationship between cropland, forest land, grassland, industrial and mining land, and changes in vegetation cover was established. Furthermore, this study projected future trends in vegetation evolution by coupling the historical trends of spatiotemporal changes in vegetation coverage in the Kuye River Basin, indicating that the risk of continuous vegetation degradation still existed in densely populated areas and regions covered by industrial and mining land. The above findings not only enrich research on the driving mechanisms of vegetation change in arid and semi-arid basins but also offer scientific support for targeted ecological restoration and land management strategies. The findings can provide scientific decision evidence for ecological governance, vegetation restoration, and long-term growth in similar regions, particularly in formulating implementation plans for mining area management and the Grain for Green program.

The outcomes of this research conformed to the patterns of vegetation change discovered by other studies on the Kuye River Basin [12], thus corroborating the reliability of the results obtained in this study. However, this study has certain limitations. A unified standard technique for spatial classification remains absent in the application of the geographic detector model. The natural breakpoint approach is widely adopted for data classification procedures, bringing prominent human subjectivity and causing imprecise identification of driving factors. Due to limitations in data availability and current technological capabilities, some potential factors, such as policy influences and mining intensity, cannot currently be obtained or quantitatively analyzed in a spatial context. Consequently, this study can only deduce the impacts of resource exploitation indirectly based on land use data. Therefore, future research should expand the scope of driving factors and establish standardized classification approaches. The Geographical Detector model reveals underlying driving

factors by detecting spatial stratified heterogeneity, which means it may not accurately infer true causal relationships. FVC is susceptible to saturation in high biomass areas, which may impact the accuracy of FVC datasets. Conversely, Enhanced Vegetation Index (EVI) data does not display significant saturation in these regions, so EVI datasets are recommended for relevant research in future studies. The absence of population density datasets prior to 2000 prevented the analysis of the effects of population density factors on changes in vegetation cover for 1986 and 1990. Due to the unavailability of land use data for 1986, data from 1980 was used as a substitute. The climate dataset has a relatively coarse spatial resolution, and the results may be affected by spatial autocorrelation. In addition, our conclusions cannot be directly extended to areas outside the Kuye River Basin. In future studies, these limitations and shortcomings should be comprehensively resolved by perfecting analytical methods and data sources to improve the precision of research outputs, thereby establishing more scientific evidence for ecological restoration and land use adjustment in arid and semi-arid regions.

5. Conclusions

Through systematic analysis of fractional vegetation cover (FVC) at 30 m resolution in the Kuye River Basin from 1986 to 2020, this study revealed the long-term evolution patterns and driving mechanisms of vegetation in arid and semi-arid basins. The results indicated that overall FVC in the basin exhibited a continuous increasing trend ($0.0105a^{-1}$). Areas with very high coverage displayed the most significant increase, whereas zones classified as very low and low coverage areas continuously decreased, indicating pronounced spatial heterogeneity. Future trend projections indicated that 91.19% of the region exhibits potential for FVC improvement. However, there remains a risk of sustained vegetation degradation in densely populated areas and regions with concentrated industrial and mining land. The driving mechanism analysis demonstrated that precipitation and land use types are the primary factors influencing changes in FVC. Land use types maintained relatively stable explanatory capacity over the long term, and their interaction with precipitation significantly strengthened the vegetation response. Further sensitivity analysis indicated that the increase in forest and grassland effectively mitigated the negative impact of cropland on moderate to high coverage areas, significantly improving the eco-environment of the Kuye River basin. Additionally, industrial and mining land had a notable impact on very low coverage areas (0–0.1). In the context of regional ecological restoration and resource exploitation, it can be inferred that the Grain for Green program and the expansion of industrial and mining land may generate differentiated impacts across diverse vegetation coverage classes. Collectively, this research further identified the multi-factor driving mechanisms of vegetation dynamics in arid and semi-arid watersheds, together with the disparate effects of various land use types on vegetation evolution. The findings offer scientific references for regional land use optimization, ecological restoration implementation, and watershed ecological security management.

Author Contributions: Conceptualization, J.Z. (Jiankang Zhang) and J.W.; Methodology, J.Z. (Jiankang Zhang), L.L. and X.D.; Software, J.Z. (Jing Zhang) and S.C.; Validation, J.Z. (Jing Zhang); Formal analysis, F.L.; Investigation, S.C.; Resources, F.L. and J.Z. (Jing Zhang); Data curation, J.Z. (Jiankang Zhang) and J.Z. (Jing Zhang); Writing—original draft, J.Z. (Jiankang Zhang); Writing—review & editing, L.L., X.D. and J.Z. (Jiankang Zhang); Visualization, X.D. and S.C.; Supervision, F.L., L.L., X.D. and J.W.; Project administration, J.W. All authors have read and agreed to the published version of the manuscript.

Funding: This research was funded by Tianjin Center, China Geological Survey (grant number DD202605101905), Institute of Ecological Conservation and Restoration, Chinese Academy of Forestry (grant number 2024ZRBSHZ094 and STSTC2023008).

Institutional Review Board Statement: Not applicable.

Informed Consent Statement: Not applicable.

Data Availability Statement: The data presented in this study are available on the data platforms listed below: Resource and Environmental Science Data Center (https://www.resdc.cn/), National Tibetan Plateau Science Data Center (http://data.tpdc.ac.cn/), Geospatial Data Cloud Platform (https://www.gscloud.cn/), National Soil Science Data Center (https://soil.geodata.cn/ztsj.html, accessed on 12 August 2025) and National Earth System Science Data Center (https://www.geodata.cn/main/, accessed on 12 August 2025).

Conflicts of Interest: The authors declare no conflict of interest.

References

1. Gu, Z.; Zhang, Z.; Yang, J.; Wang, L. Quantifying the Influences of Driving Factors on Vegetation EVI Changes Using Structural Equation Model: A Case Study in Anhui Province, China. *Remote Sens.* **2022**, *14*, 4203. [CrossRef]
2. Kong, D.; Zhang, Q.; Singh, V.P.; Shi, P. Seasonal vegetation response to climate change in the Northern Hemisphere (1982–2013). *Glob. Planet. Change* **2017**, *148*, 1–8. [CrossRef]
3. Ruan, L.; Yan, M.; Zhang, L.; Fan, X.; Yang, H. Spatial-temporal NDVI pattern of global mangroves: A growing trend during 2000–2018. *Sci. Total Environ.* **2022**, *844*, 157075. [CrossRef] [PubMed]
4. Almalki, R.; Khaki, M.; Saco, P.M.; Rodriguez, J.F. Monitoring and mapping vegetation cover changes in arid and semi-arid areas using remote sensing technology: A review. *Remote Sens.* **2022**, *14*, 5143. [CrossRef]
5. Piao, S.; Wang, X.; Park, T.; Chen, C.; Lian, X.; He, Y.; Bjerke, J.W.; Anping, C.; Philippe, C.; Tømmervik, H.; et al. Characteristics, drivers and feedbacks of global greening. *Nat. Rev. Earth Environ.* **2020**, *1*, 14–27.
6. Yao, Y.; Wang, X.; Li, Y.; Wang, T.; Shen, M.; Du, M.; He, H.; Li, Y.; Luo, W.; Ma, M. Spatiotemporal pattern of gross primary productivity and its covariation with climate in China over the last thirty years. *Glob. Change Biol.* **2018**, *24*, 184–196.
7. Li, S.; Li, X.; Gong, J.; Dang, D.; Dou, H.; Lyu, X. Quantitative Analysis of Natural and Anthropogenic Factors Influencing Vegetation NDVI Changes in Temperate Drylands from a Spatial Stratified Heterogeneity Perspective: A Case Study of Inner Mongolia Grasslands, China. *Remote Sens.* **2022**, *14*, 3320. [CrossRef]
8. Chaturvedi, R.K.; Tomlinson, K.W.; Pandey, S.K.; Tripathi, A.; Raghubanshi, A.S.; Singh, J.S. Changes in plant traits and productivity of two functional types across a soil water content gradient in a tropical dry forest. *J. Ecol.* **2025**, *113*, 3535–3549. [CrossRef]
9. Zhang, Y.; Zhang, L.; Wang, J.; Dong, G.; Wei, Y. Quantitative analysis of NDVI driving factors based on the geographical detector model in the Chengdu-Chongqing region, China. *Ecol. Indic.* **2023**, *155*, 110978. [CrossRef]
10. He, Z.; Yue, T.; Chen, Y.; Mu, W.; Xi, M.; Qin, F. Analysis of Spatial and Temporal Changes in Vegetation Cover and Driving Forces in the Yan River Basin, Loess Plateau. *Remote Sens.* **2023**, *15*, 4240. [CrossRef]
11. Xie, H.; Tong, X.; Li, J.; Zhang, J.; Liu, P.; Yu, P. Changes of NDVI and EVI and their responses to climatic variables in the Yellow River Basin during the growing season of 2000–2018. *Acta Ecol. Sin.* **2022**, *42*, 4536–4549. [CrossRef]
12. Guo, X.; Xun, X.; Liu, D.; Zhang, M.; Chen, H.; Bao, F. Impacts of Climate Change and Human Activities on Vegetation Cover during the Growing Season in the Kuye River Basin. *Trans. Chin. Soc. Agric. Eng.* **2025**, *41*, 304–313. (In Chinese)
13. Zhang, J.; Wang, J.; Shi, J. Attribution analysis of water-sediment variation under the influence of climate change and human activities in the Kuye River Basin. *Hydrogeol. Eng. Geol.* **2024**, *51*, 47–59. (In Chinese) [CrossRef]
14. Zhang, J.; Wang, J.; Zhao, N.; Shi, J.; Wang, Y. Analysis of changes in runoff and sediment load and their attribution in the Kuye River Basin of the middle Yellow River based on the slope change ratio of cumulative quantity method. *Water* **2024**, *16*, 944. [CrossRef]
15. Qiu, D.; Xu, R.; Wu, C.; Mu, X.; Zhao, G.; Gao, P. Effects of vegetation restoration on soil infiltrability and preferential flow in hilly gully areas of the Loess Plateau, China. *Catena* **2023**, *221*, 106770. [CrossRef]
16. Liu, H.; Zhang, M.; Lin, Z.; Xu, X. Spatial heterogeneity of the relationship between vegetation dynamics and climate change and their driving forces at multiple time scales in Southwest China. *Agric. For. Meteorol.* **2018**, *256–257*, 10–21. [CrossRef]
17. Kong, Z.; Ling, H.; Deng, M.; Han, F.; Yan, J.; Deng, X.; Wang, Z.; Ma, Y.; Wang, W. Past and projected future patterns of fractional vegetation coverage in China. *Sci. Total Environ.* **2023**, *902*, 166133. [CrossRef] [PubMed]
18. Huo, H.; Sun, C. Spatiotemporal variation and influencing factors of vegetation dynamics based on Geodetector: A case study of the northwestern Yunnan Plateau, China. *Ecol. Indic.* **2021**, *130*, 108005. [CrossRef]
19. Fu, F.; Zhao, M.-W.; Yang, C.; Huang, X.; Xu, Y.; Liu, Y.; Jia, S. Spatiotemporal variations of fractional vegetation cover and its response to topography on the Loess Plateau of China from 1995 to 2024. *Geomat. Nat. Hazards Risk* **2025**, *16*, 2543455. [CrossRef]

20. Mu, X.; Yin, F.; Zhang, J.; Zhang, J.; Li, W.; Liang, H.; Pei, D.; Wang, Z. Vegetation change in the Manas River Basin: Dominance of groundwater-agricultural land synergy. *Ecol. Indic.* **2025**, *180*, 114297. [CrossRef]
21. Ding, Y.; Feng, Y.; Chen, K.; Zhang, X. Analysis of spatial and temporal changes in vegetation cover and its drivers in the Aksu River Basin, China. *Sci. Rep.* **2024**, *14*, 10165. [CrossRef] [PubMed]
22. Chen, Y.; Zhao, Q.; Liu, Y.; Zeng, H. Exploring the impact of natural and human activities on vegetation changes: An integrated analysis framework based on trend analysis and machine learning. *J. Environ. Manag.* **2025**, *374*, 124092. [CrossRef]
23. Liu, C.; Li, W.; Wang, W.; Zhou, H.-k.; Liang, T.; Hou, F.; Xu, J.; Xue, P. Quantitative spatial analysis of vegetation dynamics and potential driving factors in a typical alpine region on the northeastern Tibetan Plateau using the Google Earth Engine. *Catena* **2021**, *206*, 105500. [CrossRef]
24. Li, Y.; Lei, S.; Yibo, Z.; Ruochen, C.; Penuelas, J. Vegetation dynamics and dominant driving factors in a semi-arid coal mining area under a disturbance–restoration zoning framework. *Geocarto Int.* **2026**, *41*, 2603053.
25. Li, Y.; Sun, J.; Wang, M.; Guo, J.; Wei, X.; Shukla, M.K.; Qi, Y. Spatiotemporal Variation of Fractional Vegetation Cover and Its Response to Climate Change and Topography Characteristics in Shaanxi Province, China. *Appl. Sci.* **2023**, *13*, 11532. [CrossRef]
26. Peng, W.; Kuang, T.; Tao, S. Quantifying influences of natural factors on vegetation NDVI changes based on geographical detector in Sichuan, western China. *J. Clean. Prod.* **2019**, *233*, 353–367. [CrossRef]
27. Zheng, K.; Tan, L.; Sun, Y.; Wu, Y.; Duan, Z.; Xu, Y.; Gao, C. Impacts of climate change and anthropogenic activities on vegetation change: Evidence from typical areas in China. *Ecol. Indic.* **2021**, *126*, 107648. [CrossRef]
28. Wang, X.; Hu, E.; Li, A.; Li, Q. Dynamic changes of vegetation coverage in Daqingshan Nature Reserve based on MODIS NDVI image. *J. Arid Land Resour. Environ.* **2014**, *28*, 61–65. (In Chinese)
29. Miao, Z.; Chen, J.; Wang, C.; Zhang, S.; Ma, Y.; Dong, T.; Zhao, Y.; Shi, R.; Zhao, J. Global Dynamics of Grassland FVC and LST and Spatial Distribution of Their Correlation (2001–2022). *Plants* **2025**, *14*, 439. [CrossRef] [PubMed]
30. Yang, H.; Xiong, M.; Yao, Y.X. MODIS-Based Spatiotemporal Inversion and Driving-Factor Analysis of Cloud-Free Vegetation Cover in Xinjiang from 2000 to 2024. *Sensors* **2025**, *25*, 2394. [CrossRef] [PubMed]
31. Fensholt, R.; Proud, S.R. Evaluation of Earth Observation based global long term vegetation trends—Comparing GIMMS and MODIS global NDVI time series. *Remote Sens. Environ.* **2012**, *119*, 131–147. [CrossRef]
32. Liu, Z.; Wang, H.; Li, N.; Zhu, J.; Pan, Z.; Qin, F. Spatial and Temporal Characteristics and Driving Forces of Vegetation Changes in the Huaihe River Basin from 2003 to 2018. *Sustainability* **2020**, *12*, 2198. [CrossRef]
33. Li, G.; Sun, S.; Han, J.; Yan, J.; Liu, W.; Wei, Y.; Lu, N.; Sun, Y. Impacts of Chinese Grain for Green program and climate change on vegetation in the Loess Plateau during 1982–2015. *Sci. Total Environ.* **2019**, *660*, 177–187. [CrossRef] [PubMed]
34. Mehmood, K.; Anees, S.A.; Muhammad, S.; Shahzad, F.; Liu, Q.; Khan, W.R.; Shrahili, M.; Ansari, M.J.; Dube, T. Machine Learning and Spatio Temporal Analysis for Assessing Ecological Impacts of the Billion Tree Afforestation Project. *Ecol. Evol.* **2025**, *15*, e70736. [CrossRef] [PubMed]
35. Mehmood, K.; Anees, S.A.; Rehman, A.; Pan, S.; Tariq, A.; Zubair, M.; Liu, Q.; Rabbi, F.; Khan, K.A.; Luo, M. Exploring spatiotemporal dynamics of NDVI and climate-driven responses in ecosystems: Insights for sustainable management and climate resilience. *Ecol. Inform.* **2024**, *80*, 102532. [CrossRef]
36. Tran, T.V.; Tran, D.X.; Nguyen, H.; Latorre-Carmona, P.; Myint, S.W. Characterising spatiotemporal vegetation variations using LANDSAT time-series and Hurst exponent index in the Mekong River Delta. *Land Degrad. Dev.* **2021**, *32*, 3507–3523. [CrossRef]
37. Chang, J.; Liu, Q.; Wang, S.; Huang, C. Vegetation Dynamics and Their Influencing Factors in China from 1998 to 2019. *Remote Sens.* **2022**, *14*, 3390. [CrossRef]
38. Alharbi, S.; Raun, W.R.; Arnall, D.B.; Zhang, H. Prediction of maize (*Zea mays* L.) population using normalized-difference vegetative index (NDVI) and coefficient of variation (CV). *J. Plant Nutr.* **2019**, *42*, 673–679. [CrossRef]
39. Wang, J.; Xu, C. Geodetector: Principle and Prospective. *Acta Geogr. Sin.* **2017**, *72*, 116–134. (In Chinese)
40. Yang, X.; Li, H.; Zhang, J.; Niu, S.; Miao, M. Urban economic resilience within the Yangtze River Delta urban agglomeration: Exploring spatially correlated network and spatial heterogeneity. *Sustain. Cities Soc.* **2024**, *103*, 105270. [CrossRef]
41. Jin, K.; Wang, F.; Li, P. Responses of Vegetation Cover to Environmental Change in Large Cities of China. *Sustainability* **2018**, *10*, 270. [CrossRef]
42. Cui, L.; Wang, L.; Qu, S.; Deng, L.; Wang, Z. Impacts of Temperature, Precipitation and Human Activity on Vegetation NDVI in Yangtze River Basin, China. *Earth Sci.* **2020**, *45*, 1905–1917. (In Chinese)
43. Xu, Y.; Zheng, Z.; Guo, Z.; Dou, S.; Huang, W. Dynamic Variation in Vegetation Cover and Its Influencing Factor Detection in the Yangtze River Basin from 2000 to 2020. *Environ. Sci.* **2022**, *43*, 3730–3740. (In Chinese)
44. Liu, Y.; Huang, T.; Qiu, Z.; Guan, Z.; Ma, X. Effects of precipitation changes on fractional vegetation cover in the Jinghe River basin from 1998 to 2019. *Ecol. Inform.* **2024**, *80*, 102505. [CrossRef]
45. Cheng, M.; Wang, Z.; Wang, S.; Liu, X.; Jiao, W.; Zhang, Y. Determining the impacts of climate change and human activities on vegetation change on the Chinese Loess Plateau considering human-induced vegetation type change and time-lag effects of climate on vegetation growth. *Int. J. Digit. Earth* **2024**, *17*, 2336075. [CrossRef]

46. Jiang, H.; Xu, X.; Guan, M.; Wang, L.; Huang, Y.; Jiang, Y. Determining the contributions of climate change and human activities to vegetation dynamics in agro-pastural transitional zone of northern China from 2000 to 2015. *Sci. Total Environ.* **2020**, *718*, 134871. [CrossRef]
47. Zuo, Y.; Li, Y.; He, K.; Wen, Y. Temporal and spatial variation characteristics of vegetation coverage and quantitative analysis of its potential driving forces in the Qilian Mountains, China, 2000–2020. *Ecol. Indic.* **2022**, *143*, 109429. [CrossRef]
48. Shi, S.; Wang, X.; Hu, Z.; Zhao, X.; Zhang, S.; Hou, M.; Zhang, N. Geographic detector-based quantitative assessment enhances attribution analysis of climate and topography factors to vegetation variation for spatial heterogeneity and coupling. *Glob. Ecol. Conserv.* **2023**, *42*, e02398. [CrossRef]
49. Shen, Q.; Gao, G.; Han, F.; Xiao, F.; Ma, Y.; Wang, S.; Fu, B. Quantifying the effects of human activities and climate variability on vegetation cover change in a hyper-arid endorheic basin. *Land Degrad. Dev.* **2018**, *29*, 3294–3304. [CrossRef]
50. Hao, J.; Xu, G.; Luo, L.; Zhang, Z.; Yang, H.; Li, H. Quantifying the relative contribution of natural and human factors to vegetation coverage variation in coastal wetlands in China. *CATENA* **2020**, *188*, 104429. [CrossRef]
51. Sun, Y.; Liu, S.; Liu, Y.; Dong, Y.; Li, M.; An, Y.; Shi, F.; Beazley, R. Effects of the interaction among climate, terrain and human activities on biodiversity on the Qinghai-Tibet Plateau. *Sci. Total Environ.* **2021**, *794*, 148497. [CrossRef] [PubMed]
52. Ostad-Ali-Askari, K.; Kharazi, H.G.; Shayannejad, M.; Zareian, M.J. Effect of Climate Change on Precipitation Patterns in an Arid Region Using GCM Models: Case Study of Isfahan-Borkhar Plain. *Nat. Hazards Rev.* **2020**, *21*, 04020006. [CrossRef]
53. Zhang, Y.; Jiang, X.; Lei, Y.; Gao, S. The contributions of natural and anthropogenic factors to NDVI variations on the Loess Plateau in China during 2000–2020. *Ecol. Indic.* **2022**, *143*, 109342. [CrossRef]
54. Liu, Y.; Liu, S.; Sun, Y.; Li, M.; An, Y.; Shi, F. Spatial differentiation of the NPP and NDVI and its influencing factors vary with grassland type on the Qinghai-Tibet Plateau. *Environ. Monit. Assess.* **2021**, *193*, 48. [CrossRef] [PubMed]
55. Zhao, W.; Yu, X.; Jiao, C.; Xu, C.; Liu, Y.; Wu, G. Increased association between climate change and vegetation index variation promotes the coupling of dominant factors and vegetation growth. *Sci. Total Environ.* **2021**, *767*, 144669. [CrossRef] [PubMed]

Disclaimer/Publisher's Note: The statements, opinions and data contained in all publications are solely those of the individual author(s) and contributor(s) and not of MDPI and/or the editor(s). MDPI and/or the editor(s) disclaim responsibility for any injury to people or property resulting from any ideas, methods, instructions or products referred to in the content.